EAI Endorsed Transactions
on Industrial Networks and Intelligent Systems Research Article EAI.EU

SMC-I with Approach Angle Method for Slip Suppression of Electric Vehicles

Shun Horikoshi[1], Tohru Kawabe [2,*]

[1]Department of Computer Science, Graduate School of Systems and Information Engineering, University of Tsukuba, JAPAN
[2]Division of Information Engineering, Faculty of Engineering, Information and Systems, University of Tsukuba, Tsukuba 305-8573 JAPAN

Abstract

This study presents SMC-I (sliding mode control with integral action) with approach angle method applied to slip suppression problem of electric vehicles (EVs). In SMC, chattering phenomenon always occurs through high frequency switching of the control inputs. It is undesirable phenomenon and degrade the control performance, since it causes the oscillations of the control inputs. Several studies have been conducted on this problem by introducing standard saturation function. However, studies about whether saturation function was really best weren ' t done so much. Therefore, in this paper, the SMC-I with approach angle method is proposed to improve the performance of chattering reduction and slip suppression. Then, several candidate functions for SMC are selected and both performances are compared with the proposed method. In the performance analysis, evaluation function based on the trade-off between slip suppression performance and chattering reduction performance is also proposed. The analyses are conducted in several numerical simulations of slip suppression problem of EVs.

Received on 1 September 2017; accepted on 2 December 2017; published on 21 December 2017

Keywords: Sliding mode control, Chattering, Electric vehicle, Slip suppression, Approach angle

doi:10.4108/XX.X.X.XX

1. Introduction

In this century, automobiles have become popular all over the world and the number of automobiles has been increasing rapidly, especially in the developing countries. With such wide spread of internal-combustion engine vehicles (ICEVs) all over the world, the environment and energy problems: air pollution, global warming, and so on, are going severely[1]. In this situation, therefore, the development of next-generation vehicles, for example, electric vehicles (EVs) and so on, is very important. EVs run are zero emission and eco-friendly. So EVs have attracted great interests as one of the powerful solution against the problems mentioned above [2]. EVs are driven by electric motors and electric motors have several advantages over ICEs:

1. The input/output response is faster than for gasoline/diesel engines. It is said that the motor torque response is2 orders of magnitude faster than that of the engine. E.g., if engine torque response costs 500 ms, the response time of motor toque will be 5 ms.

2. The torque generated in the wheels can be detected relatively accurately. For engine, the output torque varies along with the temperature and revolutions, even it has high-nonlinearity. Consequently, the value of torque is too difficult to be measured accurately. However, the value of motor torque is surveyed easily and accurately from the view of current control.

3. The motor can be made small enough, then the vehicles can be made smaller by using multiple motors placed closer to the wheels. The drive wheels can be controlled fully and independently.

*Corresponding author. Email: kawabe@cs.tsukuba.ac.jp

Much research has been done on the stability of general automobiles, for example, ABS (Anti-lock-Braking Systems), TCS (Traction-Control-Systems), and ESC (Electric-Stability-Control)[3] as well as VSA (Vehicle-Stability-Assist)[4] and AWC (All-Wheel-Control) [5]. What all of these have in common is that they maintain a suitable tire grip margin and reduce drive force loss to stabilize the vehicle behavior and improve drive performance. With gasoline/diesel engines, however, the response time from accelerator input until the drive force is transmitted to the wheels is slow and it is difficult to accurately determine the drive torque, which limits the vehicle's control performance.

On the other hands, EVs have a fast torque response and the motor characteristics can be used to accurately determine the torque, which makes it relatively easy and inexpensive to realize high-performance traction control. Then, several methods have been proposed for the traction control [6, 7] by using slip ratio of EVs, such as the method based on Model Following Control (MFC) in [6]. We have been proposed conventional Sliding Mode Control (SMC) based method [8].

Generally, the control performance of slip suppression by using conventional SMC [9] gets degradation due to the chattering which usually occurs by switching the SMC control inputs. The chattering is an inevitable phenomena in which the control input is oscillatory due to the structure of SMC. To overcome such disadvantages, we have also proposed the SMC-I, which adds the integral action to the sliding surface of standard SMC, in [10]. Although the slip suppression performance was fairly improved by this method, the performance of chattering reduction could not be enough. It is thought that one of the reasons for this is the fact that we employed standard saturation function for chattering reduction.

In this paper, therefore, we propose the SMC-I with approach angle (AA) [19, 20] method for improving both performance of chattering reduction and slip suppression. Then we analyze the performance compared with selected candidate functions for chattering reduction. In the analysis, evaluation function based on the trade-off between slip suppression performance and chattering reduction performance is also proposed.The analyses are conducted in several numerical simulations of slip suppression problem of EVs.

2. Sliding mode control (SMC)

2.1. Basic concept of SMC

SMC (sliding Mode Control) is one of the VSC (Variable Structure Control) method in 1970's [11, 12]. From 1980's, with the improvement of computer performance, SMC is applied in many control fields such as high-precision motor control [13], automotive control [14] and robot attitude control [15]. Now SMC is considered as an effective nonlinear-robust control method and have been attracted more and more attention. SMC utilizes discontinuous feedback control laws to force the system trajectory to reach, and subsequently to remain on a specified surface within the state space (it's so called sliding or switching surface).

For example, consider the single input nonlinear system [16]

$$x^{(n)} = f(\mathbf{x}) + b(\mathbf{x})u \tag{1}$$

where u is the control input and $\mathbf{x} = [x \quad \dot{x} \quad \dots \quad x^{(n-1)}]^T$ is the state vector. In general, the function $f(\mathbf{x})$ and the control gain $b(\mathbf{x})$ are nonlinear. In Equation (1), $f(\mathbf{x})$ and $b(\mathbf{x})$ are not exactly known, but the extents of the imprecision on $f(\mathbf{x})$ and $b(\mathbf{x})$ are upper bounded by known continuous functions of $\mathbf{x}$. The control problem is to seek a control law that makes the state $\mathbf{x}$ to track the desired state $\mathbf{x}^* = [x^* \quad \dot{x}^* \quad \dots \quad x^{*(n-1)}]^T$ in the presence of model imprecision on $f(\mathbf{x})$ and $b(\mathbf{x})$.

Let us define a time-varying surface $S(t)$ in the state space $\mathbf{R}^{(n)}$ by the equation $s(\mathbf{x}; t)$ defined as follow,

$$S(t) = \left\{x | s(\mathbf{x}; t) = 0\right\} \tag{2}$$

where $s(\mathbf{x}; t)$ is defined by

$$s(\mathbf{x}; t) = \left(\frac{d}{dt} + \alpha\right)^{n-1} \mathbf{x_e}, \ \alpha > 0 \tag{3}$$

where $\mathbf{x_e} = \mathbf{x} - \mathbf{x}^* = [x_e \quad \dot{x}_e \quad \dots \quad {x_e}^{(n-1)}]^T$ is the error between the output state and the desired state. The problem of tracking $\mathbf{x} \equiv \mathbf{x}^*$ is equivalent to remain on the surface $S(t)$ for all $t > 0$. From Equation (3), $s \equiv 0$ presents a linear differential equation whose unique solution is $\mathbf{x_e} \equiv 0$. Thus, the problem of tracking the n-dimensional vector $\mathbf{x}^*$ can be replaced by a 1st order stabilization problem in s. When $s(\mathbf{x}; t)$ equals 0, that is to say, the system trajectories reach the surface which represents the tracking error is 0. Here, $S(t)$ is known as sliding surface. On this surface, the error will converge to 0 exponentially.

This implies that if there exists a control input $u(t)$ such that $x(t)$ is in $S(t)$ and it satisfies that $x(\tau)$ is in $S(\tau)$ for all $\tau > t$, the error will converge exponentially to 0 for this control input. Figure 1 shows illustrative view of simple 2-dimensional SMC.

2.2. Implementation of SMC

In general, to design a control system based on SMC should go through the following two steps:

- Design a sliding surface that is invariant of the controlled dynamics.
- Define the control input that drives the system trajectory to the sliding surface in sliding mode in finite time.

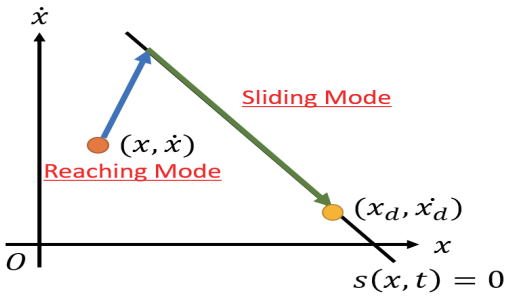

Figure 1. Graphical interpretation of SMC

Considering the system equation (1) defined in the previous section, assume that for all x, $b(\mathbf{x}) \neq 0$. We derive a control such that $\dot{s} = 0$ when the sliding mode exists, equation (3) can be rewrite as

$$s = x_e^{(n-1)} + \ldots + \alpha^{n-1} x_e. \tag{4}$$

Differentiate equation (4), we can obtain that

$$\begin{aligned} \dot{s} &= x_e^{(n)} + \ldots + \alpha^{n-1}\dot{x}_e \\ &= x^{(n)} - x^{*(n)} + \ldots + \alpha^{n-1}\dot{x}_e \\ &= f(\mathbf{x}) + b(\mathbf{x})u - x^{*(n)} + \ldots + \alpha^{n-1}\dot{x}_e \end{aligned} \tag{5}$$

while the dynamics is in sliding mode,

$$\dot{s} = 0. \tag{6}$$

By solving the equation for the control input, $u = u_{eq}$,

$$u_{eq} = \frac{1}{b(\mathbf{x})}\left(-f(\mathbf{x}) + x^{*(n)} - \ldots - \alpha^{n-1}\dot{x}_e\right). \tag{7}$$

Here, u_{eq} is called the equivalent control input, which can be interpreted as the control law that would maintain $\dot{s} = 0$ if the dynamics were in the sliding mode. However, if the system trajectory is not on the sliding surface (the reaching mode), an another item has to be added to the control input to drive the system to the sliding surface. In the reaching mode, the switching control u_{sw} makes the trajectory from the initial trajectory to the sliding surface and it can be defined as

$$u_{sw} = -\frac{K}{b(\mathbf{x})}\mathrm{sgn}(s) \tag{8}$$

where

$$\mathrm{sgn}(s) = \begin{cases} -1, & s < 0 \\ 0, & s = 0 \\ 1, & s > 0 \end{cases} \tag{9}$$

and K is called sliding gain.

In equation (8), the switching control using the discontinuous function requires infinitely fast switching, but in real systems, the sampling and delays in digital implementation causes s to pass to the other side of the surface $S(t)$, which produces chattering. Chattering is high-frequency finite oscillations which is caused by switching of the variable s around the sliding surface $S(t)$. That's the point. For reducing the chattering, it is conceivable to adopt a function $\mathrm{sat}(\frac{s}{\Phi})$ is defined as

$$\mathrm{sat}\left(\frac{s}{\Phi}\right) = \begin{cases} -1, & s < -\Phi \\ \frac{s}{\Phi}, & -\Phi \leq s \leq \Phi \\ 1, & s > \Phi \end{cases} \tag{10}$$

where $\Phi > 0$ is a design parameter representing the width of the boundary layer around the sliding surface $s = 0$. With this replacement, the sliding surface function s with an arbitrary initial value will reach and stay within the boundary layer $|s| \leq \Phi$. Figure 2 illustrates the sign function and the saturation function. From equation (8), the switching control is rewritten by

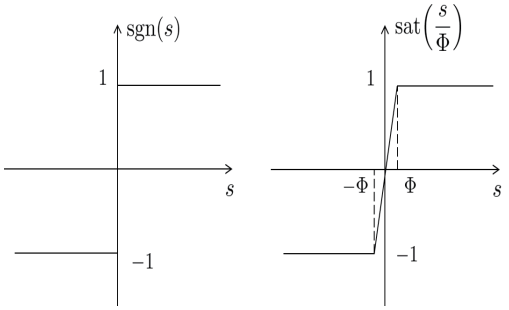

Figure 2. Sign function and saturation function

using $\mathrm{sat}(\frac{s}{\Phi})$ as

$$u_{sw} = -\frac{K}{b(\mathbf{x})}\mathrm{sat}\left(\frac{s}{\Phi}\right). \tag{11}$$

Finally, the SMC control law can be defined as

$$\begin{aligned} u &= u_{eq} + u_{sw} \\ &= \frac{-1}{b(\mathbf{x})}\left(f(\mathbf{x}) - x^{*(n)} + \ldots + \alpha^{n-1}\dot{x}_e + K\mathrm{sat}\left(\frac{s}{\Phi}\right)\right). \end{aligned} \tag{12}$$

In summary, when the trajectory is on the sliding surface ($s = 0$), it is desired to have $u_{sw} = 0$, the switching control has no effect on the sliding surface. Moreover, when the trajectory is off the sliding surface or the uncertainty in the system occurs, the switching control acts to return the trajectory back to the sliding surface. Therefore, the total control u causes the system to keep the trajectory on the sliding surface.

3. Electric Vehicle Dynamics

3.1. One weel car model

As a first step toward practical application, this paper restricts the vehicle motion to the longitudinal direction and uses direct motors for each wheel to simplify the one-wheel model to which the drive force is applied. In addition, braking was not considered this time with the subject of the study being limited to only when driving.

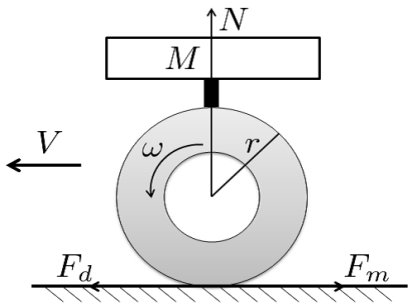

Figure 3. One-wheel car model

From fig. 3, the vehicle dynamical equations are expressed as eqs. (13) to (15).

$$M\frac{dV}{dt} = -F_d(\lambda) + F_a \tag{13}$$

$$J\frac{d\omega}{dt} = rF_d(\lambda) - T_b \tag{14}$$

$$F_d = \mu(c,\lambda)N \tag{15}$$

where M is the vehicle weight, V is the vehicle body velocity, F_d is the driving force, J is the wheel inertial moment, F_a is the resisting force from air resistance and other factors on the vehicle body, T_b is the braking torque, ω is the wheel angular velocity, r is the wheel radius, c is road surface condition coefficient, and λ is the slip ratio. The slip ratio of the wheel is defined as the difference between the wheel and body velocities, divided by the maximum of these velocity values (wheel velocity for acceleration, vehicle body velocity for braking), and given by

$$\lambda = \begin{cases} \dfrac{V_\omega - V}{V_\omega} & \text{(accelerating)} \\ \dfrac{V - V_\omega}{V} & \text{(braking)} \end{cases} \tag{16}$$

The value of $\lambda = 0$ characterizes the free motion of the wheel where no wheel slip happens (no friction force is exerted). If the slip attains the value $\lambda = 1$, then the wheel is completely skidding. The friction forces that are generated between the road surface and the tires are the force generated in the longitudinal direction of the tires and the lateral force acting perpendicularly to the vehicle direction of travel, and both of these are expressed as a function of λ. The friction force generated in the tire longitudinal direction is expressed as μ, and the relationship between μ and λ is shown by equation (17) below, which is a formula called the **Magic-Formula** and gives values compatible with experimental data given in [17]. It is simplified and has been using in earlier study in [18].

$$\mu(c,\lambda) = -c \times 1.1 \times \left(e^{-35\lambda} - e^{-0.35\lambda}\right) \tag{17}$$

where c is the coefficient used to determine the road condition and was found by experimental data to be approximately $c = 0.8$ for general dry asphalt roads, approximately $c = 0.5$ for general wet asphalt roads, and approximately $c = 0.12$ for icy road. In the simulations, this formula is used for estimating the maximum value of friction coefficient.

The $\mu - \lambda$ curve for acceleration case is shown in figure 4 on three different road conditions (dry asphalt, wet asphalt and icy road). It shows how the friction coefficient μ increases with slip ratio λ up to a value λ^* $(0.1 < \lambda^* < 0.2)$ where it attains the maximum value of the friction coefficient. As defined in equation (15), the driving force also achieves the maximum value in corresponding to the friction coefficient. However, the friction coefficient decreases to the minimum value when the wheel is completely skidding. Therefore, to achieve the maximum value of driving force for slip suppression, λ should be maintained at the desired value λ^*. The value of λ^* is derived as follows.

Choose the function $\mu_c(\lambda)$ defined as

$$\mu_c(\lambda) = -1.1 \times \left(e^{-35\lambda} - e^{-0.35\lambda}\right). \tag{18}$$

By using equation (18), Equation (17) can be rewritten as

$$\mu(c,\lambda) = c \cdot \mu_c(\lambda). \tag{19}$$

Evaluating the values of λ which maximize $\mu(c,\lambda)$ for different $c(c > 0)$, means to seek the value of λ where the maximum value of the function $\mu_c(\lambda)$ can be obtained. Then let

$$\frac{d}{d\lambda}\mu_c(\lambda) = 0 \tag{20}$$

and solving Equation (20) gives

$$\lambda = \frac{log100}{35 - 0.35} \approx 0.13. \tag{21}$$

Therefore, for the different road conditions, when $\lambda \approx 0.13$ is satisfied, the maximum driving force can be gained. Namely, from Equation (17) combined with figure 4 we find that regardless of the road condition (value of c), the $\mu - \lambda$ surface attains the largest value of μ when λ is the optimal value 0.13. So in this dissertation, desired value of slip ratio is set by $\lambda^* = 0.13$.

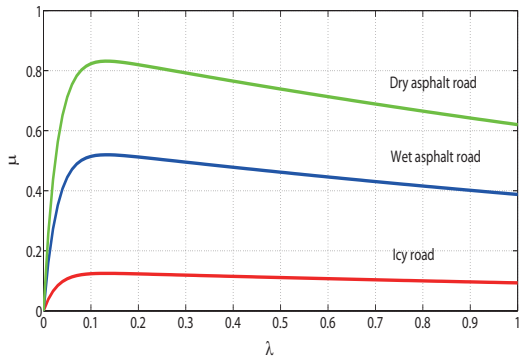

Figure 4. $\mu - \lambda$ curve

4. SMC with Integral Action for Slip Suppression

In this section, the previous proposed control strategy based on SMC with integral action (SMC-I) [10] is explained. Without loss of generality, one wheel car model in fig. 3 is used for the design of the control law. The nonlinear system dynamics can be presented by a differential equation as

$$\dot{\lambda} = f + bT_m \tag{22}$$

where $\lambda \in R$ is the state of the system representing the slip ratio of the driving whee which is defined as equation (16) for the case of acceleration, $T_m \in R$ is the control input representing the torque of the motor. f describes the nonlinearity of system and b is the input gain, and they are all time-varying. Differentiating equation (16) for the case of acceleration with respect to time gives

$$\dot{\lambda} = \frac{-\dot{V} + (1-\lambda)\dot{V}_w}{V_w} \tag{23}$$

Then, the system dynamics can be rewritten as

$$\dot{\lambda} = -\frac{g}{V_w}\left[1 + (1-\lambda)\frac{r^2 M}{J_w}\right]\mu(c,\lambda) + \frac{(1-\lambda)r}{J_w V_w}T_m. \tag{24}$$

By reference to the system dynamics, the following equations can be attained,

$$f = -\frac{g}{V_w}\left[1 + (1-\lambda)\frac{r^2 M}{J_w}\right]\mu(c,\lambda), \tag{25}$$

$$b = \frac{(1-\lambda)r}{J_w V_w}. \tag{26}$$

The sliding mode controller is described to maintain the value of slip ratio λ at the desired value λ^*.

Referring to [10], in order to reduce the undesired chattering effect for which it is possible to excite high frequency modes, and guarantee zero steady-state error, an integral action with gain has been introduced to the design of sliding surface. By adding an integral item to the difference between the actual and desired values of the slip ratio, the sliding surface function s is given by

$$s = \lambda_e + K_{in}\int_0^t \lambda_e(\tau)d\tau, \tag{27}$$

where λ_e is defined as $\lambda_e = \lambda - \lambda^*$ and K_{in} is the integral gain, $K_{in} > 0$.

The sliding mode occurs when the state reaches the sliding surface defined by $s = 0$. The dynamics of sliding mode is governed by

$$\dot{s} = 0. \tag{28}$$

By using eqs. (22) to (28), the sliding mode control law is derived by adding a switching control input T_{msw} to the nominal equivalent control input T_{meq_n} as in [10]

$$T_m = T_{meq\_n} + T_{msw}, \tag{29}$$

$$T_{meq\_n} = \frac{1}{b}\left[-f_n - K_{in}\lambda_e\right], \tag{30}$$

$$T_{msw} = \frac{1}{b}\left[-K\mathrm{sat}(\frac{s}{\Phi})\right], \tag{31}$$

$$\mathrm{sat}\left(\frac{s}{\Phi}\right) = \begin{cases} -1 & s < -\Phi \\ \frac{s}{\Phi} & -\Phi \le s \le \Phi, \\ 1 & s > \Phi \end{cases} \tag{32}$$

where " $_n$ " is used to indicate the estimated model parameters. f_n is the estimation of f calculated by using the nominal values of vehicle mass M_n and road surface condition coefficient c_n. $\Phi > 0$ is a design parameter which defines a small boundary layer around the sliding surface. The sliding gain $K > 0$ is selected as

$$K = F + \eta \tag{33}$$

by defining Lyapunov candidate function in [10], where $F = |f - f_{\_n}|$ and η is a design parameter.

By using eqs. (29), (30), (31) and (33), the control law of SMC-I can be represented as

$$T_m = \frac{1}{b}\left[-f_n - K_{in}\lambda_e - (F+\eta)\mathrm{sat}\left(\frac{s}{\Phi}\right)\right]. \tag{34}$$

In this method, standard saturation function, $\mathrm{sat}\left(\frac{s}{\Phi}\right)$ in equation (32), was employed for chattering reduction.

5. SMC-I with approach angle method

To improve the performances of chattering reduction and slip suppression of SMC-I in equation (10), we introduce the approach angle (AA) [19, 20] . AA means

approaching angle of state trajectory to the sliding surface as shown in figure 5. Larger value of AA means quicker approaching of state trajectory to the surface. In such case, the control input becomes more oscillatory. On the other hand, smaller value of AA means gentler approaching of it. So, the oscillation of the control input is small.

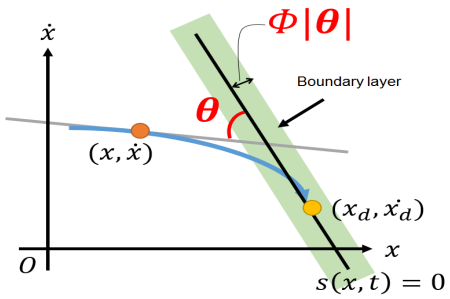

Figure 5. Schematic views of phase trajectory of λ(blue arrow) and its tangent line(gray line).

From figure 5 and state-space equation (22), the tangent line of the state trajectory at the current time ($t = T$) is described as

$$\dot{\lambda} - \dot{\lambda}(T) = \ddot{\lambda}(T)(\lambda - T) \tag{35}$$

This is the gray-line in the figure 5. Then, the normal vector of the trajectory is

$$(\ddot{\lambda}(T), -1) \tag{36}$$

From time differential of the sliding surface in equation(27),

$$\dot{\lambda} + K_i\lambda = 0 \tag{37}$$

is obtained. Then, the normal vector of the sliding surface is

$$(K_i, 1) \tag{38}$$

We can obtain the value of AA (θ) from these as follows.

$$\theta = cos^{-1}\frac{|K_i\ddot{\lambda}(T) - 1|}{\sqrt{\ddot{\lambda}(T)^2 + 1}\sqrt{K_i^2 + 1}} \tag{39}$$

Finally, the saturation function with AA is defined as

$$\mathrm{sat}_{AA}\left(\frac{s}{\Phi}, \theta\right) = \begin{cases} -1 & (s < -\Phi|\theta|) \\ \frac{s}{\Phi|\theta|} & (-\Phi \le s \le \Phi|\theta|) \\ 1 & (s > \Phi|\theta|) \end{cases} \tag{40}$$

By using this, the control input of SMC-I in equation (34) is changed as

$$T_m = \frac{1}{b}\left[-f_n - K_{in}\lambda_e - (F + \eta)\mathrm{sat}_{AA}\left(\frac{s}{\Phi}\right)\right]. \tag{41}$$

This is the proposed SMC-I with AA method.

6. Analysis of Control Performance

6.1. Other chattering functions

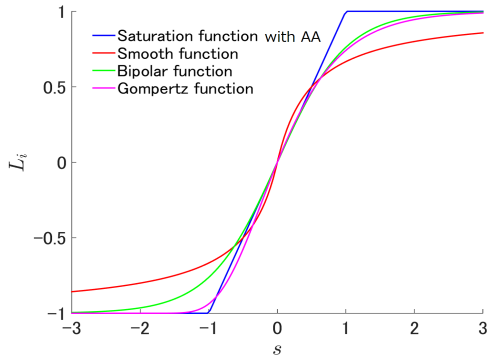

Figure 6. Candidate functions.

The switching control input using the sign function in equation (9) is used theoretically. But, in real systems, the sampling and delays in digital implementation causes s to pass to the other side of the surface $S(t)$, which produces chattering. A solution to reduce this chattering introduces a region around $S(t)$ called boundary layer so that s changes its value continuously [16]. The boundary layer is realized to use "S-shape type" function replacing sgn(s). Since the trajectory in the boundary layer varies depend on the used function, the chattering reduction performance is different. Hereinafter the function of the S-shape type used for boundary layer introduction is called the chattering reduction function. In this paper, L_0, L_1, L_2 and L_3 shown in equation (45) are considered as candidates of the chattering function,

$$L_0 = \begin{cases} -1 & (s < -\Phi|\theta|) \\ \frac{s}{\Phi|\theta|} & (-\Phi \le s \le \Phi|\theta|) \\ 1 & (s > \Phi|\theta|) \end{cases} \tag{42}$$

$$L_1 = \frac{s}{|s| + \delta} \tag{43}$$

$$L_2 = \tanh\left(\frac{\sigma s}{2}\right) \tag{44}$$

$$L_3 = 2 \times \left(\frac{1}{2}\right)^{b^s} - 1 \tag{45}$$

where Φ, δ, σ, $b(0 < b < 1)$ are design parameters related to the width of boundary layer.

L_0 is Saturation function with AA, and it's same as equation (40). In this function, the width of the boundary layer becomes narrow so as to smaller the value of Φ. L_1 is Smooth function. In this function, the width of the boundary layer becomes narrow so as to smaller the value of δ. L_2 is Bipolar function. In this function, the width of the boundary layer becomes narrow so as to bigger the value of σ. L_3 is Gompertz

function and its asymmetry. In this function, the width of the boundary layer becomes narrow so as to smaller the value of b. The chattering reduction performance of these four functions are analyzed. These four functions are shown in figure 6. Values of parameters in each function are tuned as $\Phi = 1.0, \delta = 0.5, \sigma = 2.0, b = 0.2$ for visibility.

6.2. Evaluation Index for Control Performance

The index to compare the performance of 4 candidate functions is considered. It can be said that there is generally a relation of a trade-off in the slip suppression performance and the chattering reduction performance in slip suppression problem by using SMC. Therefore, it is desirable to reduce chattering of the driving torque without deteriorating slip suppression performance. From this fact, the following evaluation index is introduced.

$$J = k_c C + k_e E \tag{46}$$

where $C = \max\left|\frac{dT_m}{dt}\right|$, $E = \int_0^{t_f} |\tilde{\lambda}| dt$ and where k_c and k_e are design parameters. C is a maximum value of gradient of driving torque. The amplitude of the vibration of the driving torque could be gently suppressed small by holding down of C small. In other words, smaller value of C means higher chattering reduction performance. On the other hands, E indicates the accumulated error with the value and the target value of slip rate from simulation starting to the end. Namely, smaller value of E means higher slip suppression performance.

Then, the chattering reduction performance and slip suppression performance of L_0, L_1, L_2 and L_3 are analyzed by calculating the minimum value of this J with changing the value of parameters in these functions, Φ, δ, σ, b, respectively.

6.3. Performance Analysis by Simulations

In simulations, we consider three different road conditions, a dry asphalt, a wet asphalt and an icy road. As the input to the simulation of system, the driving torque is produced by the constant pressure on the accelerator pedal, which is decided on the vehicle speed desired by the driver. Here, the vehicle speed is desired to achieve $180[km/h]$ in $15[s]$ by a fixed acceleration after starting the car. The range of variation in mass of vehicle M and road condition coefficient c are imposed as $M_{max} = 1400[kg]$, $M_{min} = 1000[kg]$, $c_{max} = 0.9$ and $c_{min} = 0.1$ respectively. So the nominal values of mass and road condition coefficient can be obtained as $\hat{M} = 1200[Kg]$ and $\hat{c} = 0.5$.

The values of design parameters are set as Table 1. These values are obtained by trial and error search in preliminary simulations and they lowered the value of J.

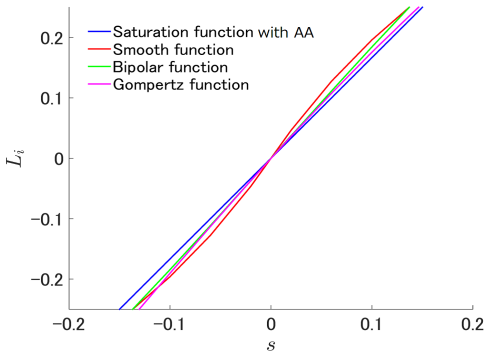

Figure 7. Candidate functions on dry asphalt simulation.

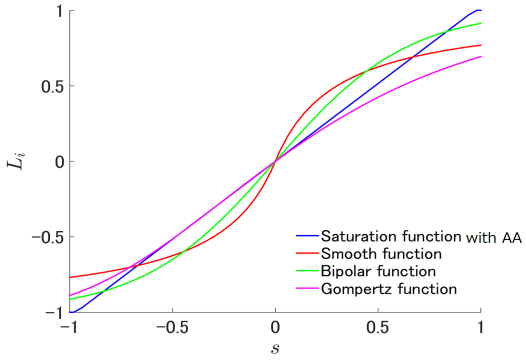

Figure 8. Candidate functions on wet asphalt simulation

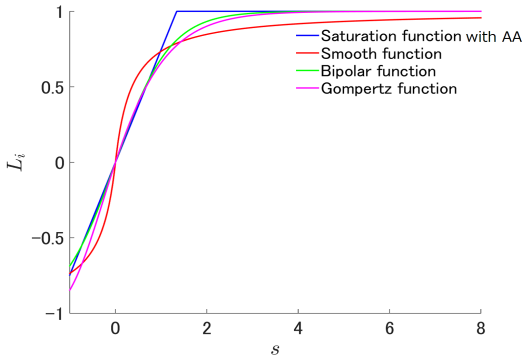

Figure 9. Candidate functions on icy road.

Table 1. Parameters of each candidate functions.

	Dry	Wet	Icy
Φ in Saturation function(L_0)	0.60	0.97	1.34
δ in Smooth function(L_1)	0.41	0.30	0.36
σ in Bipolar function(L_2)	3.73	3.10	1.68
b in Gompertz function(L_3)	0.07	0.24	0.27

[a] *Results on dry asphalt*($c = 0.8$)

Time responses of driving torque and slip ratio on dry asphalt are shown in figures 10 and 11 respectively. The difference can't be understood so much, so the one into which the first section($0 < t < 0.05$) with the conspicuous difference was expanded is indicated in figures 12 and 13.

From these figures, we can see that the time responses of driving torque and slip ratio with all functions hardly have the difference, and their both chattering reduction performance and control performance may be almost equal.

[b] *Results on wet asphalt($c = 05$)*

Time responses of driving torque and slip ratio on wet asphalt are shown in figures 14 and 15 respectively. The difference can't be understood so much, so the one into which the first section($0 < t < 0.05$) with the conspicuous difference was expanded is indicated in figures 16 and 17.

From these figures, we can see that there is no big difference in the chattering reduction performance. But, we see the time responses of driving torque and slip ratio with gompertz function are slightly inferior to other functions, especially in first transient section. It shows slow convergence compared with the other functions. Smooth function is slightly good among all.

[c] *Results on icy road($c = 0.12$)*

Time responses of driving torque and slip ratio on icy road are shown in figures 18 and 19 respectively. The difference can't be understood so much, so the one into which the first section($0 < t < 0.05$) with the conspicuous difference was expanded is indicated in figures 20 and 21.

From these figures, also we can not see the difference in the chattering reduction. The time responses of driving torque with saturation function seems to be slightly bad, since it shows large oscillatory reaction compared with the other functions, especially in first transient section. On the other hands, saturation function with AA shows superior response in both response of driving torque and slip ratio to other functions.

[d] *Discussion*

Although there is difference according to the road surface conditions, it can maybe said that saturation function is excellent overall from simulation results of [a], [b] and [c]. The reason is considered from the shape of each function.

Firstly, figure 7 shows the shape of each function on dry asphalt simulation. From this figure, we can see that there is almost no difference among these functions. Therefore, the effect of each function is almost same, especially in the chattering reduction.

Next, figure 8 shows the shape of each function on wet asphalt simulation. In this case, the absolute values of gompertz function in the section of $s > 0.5$ are smaller than the other functions. Namely, the values of gomperz function away from the top value. compared with other functions. Therefore, the effect of bringing the state close to the switching surface is weak. This makes bigger the value of E in J and worse the performance of slip suppression. On the other hands, smooth function has bigger value than the one of other functions at the around of $s = -1$ and the rate of change is big through the whole compared with others. It seems that this well-controlled change of saturation function with AA makes goof effect to performances of driving torque and slip ratio.

Finally, figure 9 shows the shape of each function on icy road simulation. From this figure, we can see that the saturation function strictly reach the value of 1 rather faster than other functions. Other functions do not reach the value of 1 strictly. This means that the effect of bringing the state close to the switching surface of the other functions is rather weak than the one of saturation function with AA. Therefore, the saturation function shows superior performance of slip suppression among all.

7. Conclusion

In this paper, we proposed the SMC-I with AA method for improving the performance of chattering reduction and slip suppression in motion control problem of EVs. Then, to analyze this method, the performance compared with selected 3 candidate functions ,smooth function (L_1), bipolar function (L_1) and gompertz function (L_3) , for chattering reduction. The evaluation index (J) taking into the trade-off relation in the slip suppression performance and the chattering reduction performance is also proposed for this purpose. We analyze the control performance of SMC-I with 4 functions by this index from simulations with three different road conditions, a dry asphalt, a wet asphalt and an icy road. As a result, we can see that there is no big difference of 4 functions in chattering reduction performance. and that saturation function with AA shows somewhat good performance relatively, especially in slip suppression performance. In future works, therefore, it is need to extend the SMC-I with AA method to become more practical, for example, introducing the low-pass filter to AA and so on.

Acknowledgements

This research was partially supported by Grant-in-Aid for Scientific Research (C) (Grant number: 16K06409; Tohru Kawabe; 2016-2018) from the Ministry of Education, Culture, Sports, Science and Technology of Japan.

References

[1] A.G. Mamalis, K.N. Spentzas and A.A. Mamali, The Impact of Automotive Industry and Its Supply Chain

to Climate Change: Somme Techno-economic Aspects, *European Transport Research Review*, Vol.5, No.1, 2013, pp.1–10.

[2] H. Tseng and J.S. Wu and X. Liu, Affordability of Electric Vehicle for a Sustainable Transport System: An Economic and Environmental Analysis, *Energy Policy*, Vol.61, 2013, pp.441–447.

[3] A.T. Zanten, R. Erhardt and G. Pfaff, VDC; The Vehicle Dynamics Control System of Bosch, *Proc. Society of Automotive Engineers International Congress and Exposition*, 1995, Paper No. 950759.

[4] K. Kin, O. Yano and H. Urabe, Enhancements in Vehicle Stability and Steerability with VSA, *Proc. JSME TRANSLOG 2001*, 2001, pp.407–410 (in Japanese).

[5] K. Sawase, Y. Ushiroda and T. Miura, Left-Right Torque Vectoring Technology as the Core of Super All Wheel Control (S-AWC), *Mitsubishi Motors Technical Review* , No.18, 2006, pp.18–24 (in Japanese).

[6] S. Kodama, L. Li and H. Hori, Skid Prevention for EVs based on the Emulation of Torque Characteristics of Separately-wound DC Motor, *Proc. The 8th IEEE International Workshop on Advanced Motion Control*, VT-04-12, 2004, pp.75–80.

[7] K. Fujii and H. Fujimoto, Slip ratio control based on wheel control without detection of vehicle speed for electric vehicle, *IEEJ Technical Meeting Record*, VT-07-05, 2007, pp.27–32 (in Japanese).

[8] S. Li, K. Nakamura, T. Kawabe and K. Morikawa, A Sliding Mode Control for Slip Ratio of Electric Vehicle, *Proc. of SICE Annual Conference 2012*, pp.1974–1979.

[9] I. Eker and A. Akinal, Sliding Mode Control with Integral Augmented Sliding Surface: Design and Experimental Application to an Electromechanical system, *Electrical Engineering*, Vol.90, 2008, pp.189–197.

[10] S. Li and T. Kawabe, Slip Suppression of Electric Vehicles Using Sliding Mode Control Method, *International Journal of Intelligent Control and Automation*, Vol.4, No.3, 2013, pp.327–334.

[11] V. Utkin, Variable Structure Systems with Sliding Modes, *IEEE Transactions on Automatic Control*, Vol. 22, No. 2, 1977, pp. 212-222.

[12] V. Utkin, *Sliding Modes and Their Applications in Variable Structure Systems*, Mir Publishers, USSR, 1978.

[13] U. M. Ch, Y. S. K. Babu and K. Amaresh, Sliding Mode Speed Control of a DC Motor, *Proc. of 2011 International Conference on Communication Systems and Network Technologies*, 2011, pp. 387-391.

[14] K. Nakano, U. Sawut, K. Higuchi and Y. Okajima, Modelling and Observer-based Sliding-mode Control of Electronic Throttle Systems, *Transaction on Electrical Engineering, Electronics and Communications*, Vol. 4, No. 1, 2006, pp. 22-28.

[15] Y. Li, J. O. Lee and J. Lee, Attitude Control of the Unicycle Robot Using Fuzzy-sliding Mode Control, *Proc. of the 5th International Conference on Intelligent Robotics and Applications*, Vol. 3, 2012, pp. 62-72.

[16] J. E. Slotine, W. Li, *Applied Nonlinear Control*, Prentice Hall, 1991, USA.

[17] H. B. Pecejka and E. Bakker, The Magic Formula Tyre Model, *Proc. of the 1st International Colloquium on Tyre Models for Vehicle Dynamics Analysis*, 1991, pp. 1-18.

[18] Y. Hori, Simulation of MFC-Based Adhesion Control of 4WD Electric Vehicle, *IEEJ Record of Industrial Measurement and Control*, Vol. IIC-00, No. 1-23, 2000, pp. 67-72 (in Japanese).

[19] M. R. Rafimanzelat and M. J. Yazdanpanah, A Novel Low Chattering Sliding Mode Controller, *The Proc. of the 2004 5th Asian Control Conference*. Vol.3, 2004, pp.1958-1963 (DOI:10.1109).

[20] Kenneth R. Buckholtz, Approach Angle-Based Swtiching Function for Sliding Mode Control Design, *The Proc. of the 2002 American Control Conference*, Vol.3, 2002, pp.2368-2373.

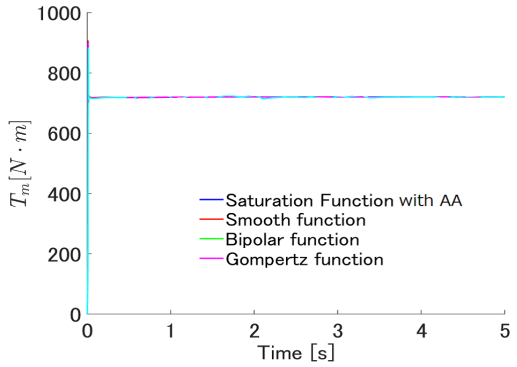

Figure 10. Time response of driving torque on dry asphalt

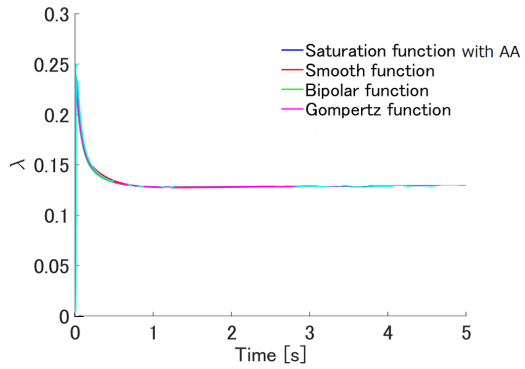

Figure 11. Time response of slip ratio on dry asphalt

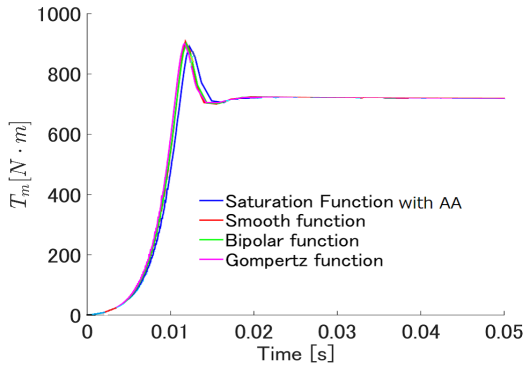

Figure 12. Enlarged view of time response of driving torque on dry asphalt ($(0 < t < 0.05)$

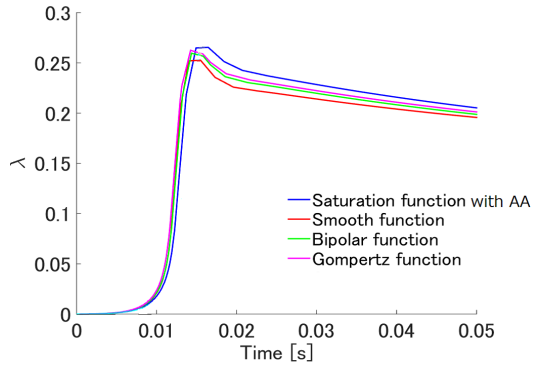

Figure 13. Enlarged view of time response of slip ratio on dry asphalt ($(0 < t < 0.05)$

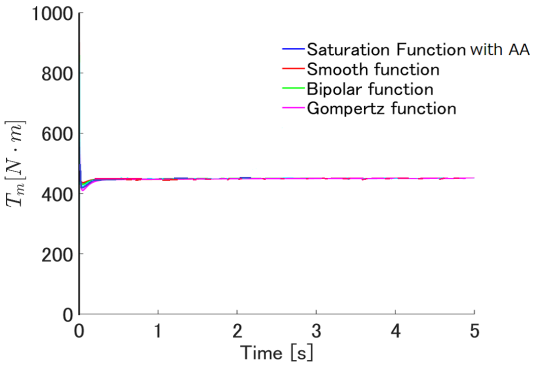

Figure 14. Time response of driving torque on wet asphalt

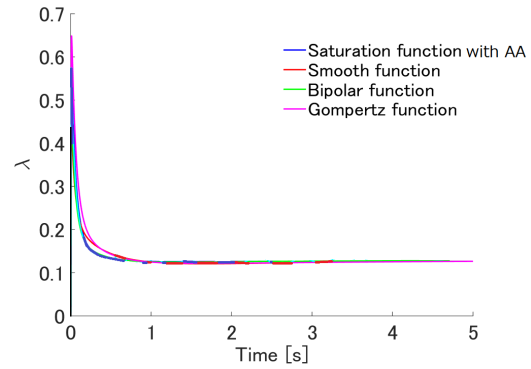

Figure 15. Time response of slip ratio on wet asphalt

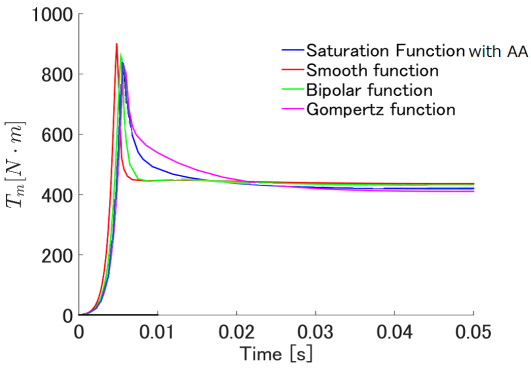

Figure 16. Enlarged view of time response of driving torque on wet asphalt ($(0 < t < 0.05)$

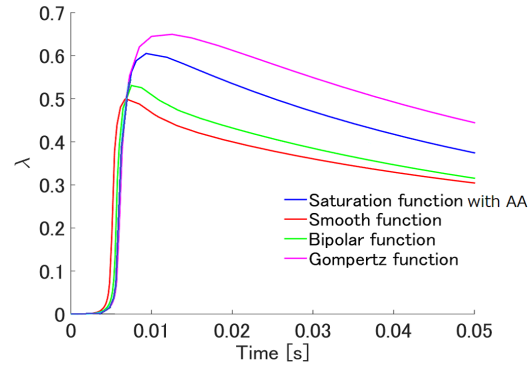

Figure 17. Enlarged view of time response of slip ratio on wet asphalt ($(0 < t < 0.05)$

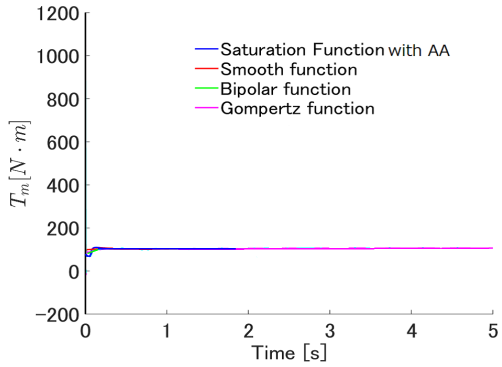

Figure 18. Time response of driving torque on icy road

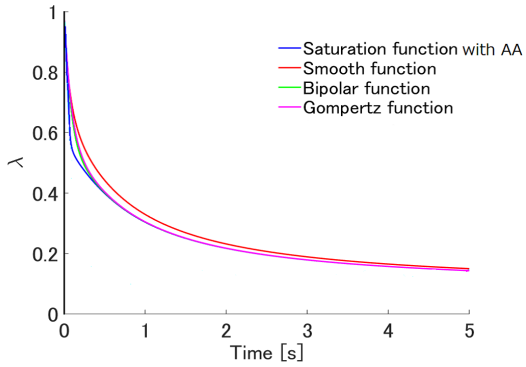

Figure 19. Time response of slip ratio on icy road

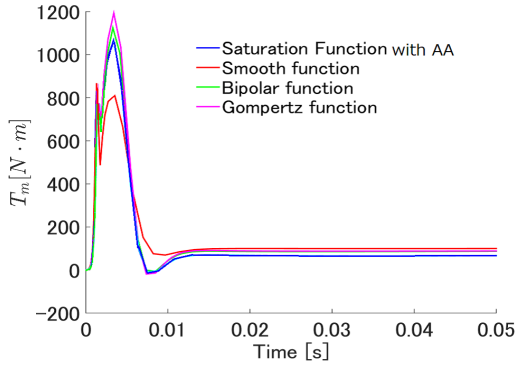

Figure 20. Enlarged view of time response of driving torque on icy road ($(0 < t < 0.05)$

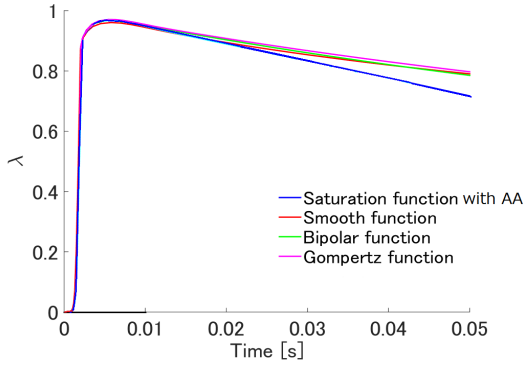

Figure 21. Enlarged view of time response of slip ratio on icy road ($(0 < t < 0.05)$